

The Mixed Spin $S = (\frac{1}{2}, 1)$ XXZ Ferrimagnet at Zero Temperature

Weihong Zheng* and J. Oitmaa†

School of Physics, The University of New South Wales, Sydney, NSW 2052, Australia.

(Dated: March 22, 2022)

Linked cluster series expansions about the Ising limit are used to study ground state properties, viz. ground state energy, magnetization and excitation spectra, for mixed spin $S = (\frac{1}{2}, 1)$ quantum ferrimagnets on simple bipartite lattices in 1, 2, and 3-dimensions. Results are compared to second-order spin wave theory and, in general, excellent agreement is obtained.

I. INTRODUCTION

Ferrimagnets are materials where ions on different sublattices have opposing magnetic moments which do not cancel in the ordered phase¹. This can arise either through unequal numbers of ions on the sublattices or the ions having different spin quantum numbers. There is growing interest in such systems, both from fundamental physics and through their technological potential. Arguably the simplest such structures are bipartite lattices (A,B) with $S_A \neq S_B$, with nearest neighbour antiferromagnetic exchange coupling. The experimental discovery of ferrimagnetism in bimetallic chains² has led to many studies of mixed-spin chains^{3,4,5}. The rare-earth nickelates $R_2\text{BaNiO}_5$ ⁶, which can be modelled by a 2-dimensional net of coupled chains^{7,8}, are an example of a mixed-spin system in 2-dimensions. Another example is an Fe-Ni cyanide bridged network⁹, which provides a realization of the square lattice model we consider in this paper.

We consider, in this paper, the cases of a bipartite chain, square lattice, and simple-cubic lattice where sublattice A is occupied by $S = \frac{1}{2}$ spins and sublattice B by $S = 1$ spins, with nearest neighbour antiferromagnetic coupling between the sublattices. This is the extreme quantum limit, where quantum fluctuations will be most significant. The Hamiltonian is taken as

$$H = J \sum_{\langle ij \rangle} [s_i^z S_j^z + \frac{x}{2} (s_i^+ S_j^- + s_i^- S_j^+)] \quad (1)$$

where the parameter $0 < x < 1$ represents exchange anisotropy, the coupling $J > 0$ and it can be set to be 1.

Previous work on this system includes spin-wave theory¹⁰, and a variety of systematic numerical methods^{3,4,5}, with most emphasis on the mixed-spin chain. Other work has included frustrating further neighbour interactions for the chain¹¹ and square lattice¹², but we do not consider such cases here.

Our approach is to use high-order linked-cluster expansions¹³, where quantities are expanded about the Ising limit as power series in x , a technique we have employed in previous studies of quantum antiferromagnets¹⁴. This allows the whole region $0 < x < 1$ to be studied, as well as extrapolation to the isotropic Hamiltonian $x = 1$. In particular we compute series for the ground state energy, the magnetization on each sublattice, and the dispersion relations for magnon excitations.

Since we will compare the series predictions with spin-wave theory, we provide here the relevant spin-wave results at lowest order, for the general case with spins S_1 and S_2 . Further details, including the second-order results, are given in the Appendix. The ground state energy and magnetizations are

$$E_0/NJ = -zS_1S_2/2 + \frac{z}{2N} \sum_{\mathbf{k}} [\sqrt{(S_1 + S_2)^2 - 4S_1S_2x^2\gamma_{\mathbf{k}}^2} - (S_1 + S_2)] \quad (2)$$

$$M_{1,2} = S_{1,2} - \frac{1}{N} \sum_{\mathbf{k}} \left[\frac{S_1 + S_2}{\sqrt{(S_1 + S_2)^2 - 4S_1S_2x^2\gamma_{\mathbf{k}}^2}} - 1 \right] \quad (3)$$

where the sum is over $N/2$ \mathbf{k} -values in the reduced Brillouin zone, z is the lattice coordination number, and $\gamma_{\mathbf{k}}$ is the usual factor $\gamma_{\mathbf{k}} = \frac{1}{z} \sum_{\delta} e^{i\mathbf{k} \cdot \delta}$. The first term in (2), (3) is the classical result, and the second term is the lowest correction due to quantum fluctuations.

The two branches of magnon energies are given by

$$\omega_{\mathbf{k}}^{\pm} = \frac{1}{2} z J \left[\sqrt{(S_1 + S_2)^2 - 4S_1S_2x^2\gamma_{\mathbf{k}}^2} \pm (S_2 - S_1) \right] \quad (4)$$

The most interesting feature of these is that, at $x = 1$, one branch is gapped, while the other becomes gapless but with quadratic dispersion

$$\left. \begin{aligned} \omega_{\mathbf{k}}^{+} &\simeq zJ(S_2 - S_1) \\ \omega_{\mathbf{k}}^{-} &\simeq \text{const. } k^2 \end{aligned} \right\} \quad \mathbf{k} \rightarrow 0 \quad (5)$$

This result is well known, and is a consequence of $S_1 \neq S_2$. Another feature, which we have not seen commented on previously, is that the various quantities are analytic at $x = 1$, unlike the case of the usual antiferromagnet, where there are square root singularities. This makes the extrapolation of our series to $x = 1$ much more precise.

The outline of the paper is as follows. In Section II we give (brief) details of our method and present some of the raw data. In Section III we present an analysis, mainly in graphical format, for 1, 2 and 3-dimensions. The spin wave results are shown for comparison. We find that many of our results agree extremely well with second-order spin-wave theory, and are indistinguishable on the scale of the figures. In Section IV we present some conclusions.

II. DERIVATION OF SERIES EXPANSIONS

The series are obtained, as described in ref.[13], by evaluating the “proper” or “cumulant” contribution for each of a set of connected clusters, and then summing these, with their respective embedding factors, to obtain the series for the bulk system. In this way the ground state energy per site, for example, is written in the form

$$E_0/NJ = \sum_{n=0}^{\infty} e_n x^n \quad (6)$$

where the purely numerical coefficients e_n are computed exactly to some maximum order (in this work, to order 22, 14, 12 for $d = 1, 2, 3$ respectively). The coefficients are given in Table I, for the case $S_1 = \frac{1}{2}$, $S_2 = 1$, which is the only case we consider. Table II gives the corresponding coefficients for the magnetization series. We note that, apart from the constant term, these series are identical and hence only M_1 is given.

Series for the excitation spectra are obtained via the linked cluster method of Gelfand (see [13]), in which we write

$$\omega(\mathbf{k}) = \sum_{\mathbf{R}} t(\mathbf{R}) e^{i\mathbf{k} \cdot \mathbf{R}} \quad (7)$$

where the $t(\mathbf{R})$ are a set of “transition weights” obtained from an effective Hamiltonian. The series for two branches of excitation spectra has been computed upto order 22, 10, 8 for $d = 1, 2, 3$ respectively, which involve a list of 22, 185928, 59804 clusters, respectively. In Table II we provide our results for these, for the square lattice. In Table I, we also list the series for excitation spectra at $\mathbf{k} = 0$ for all three lattices. We are happy to provide other results on request.

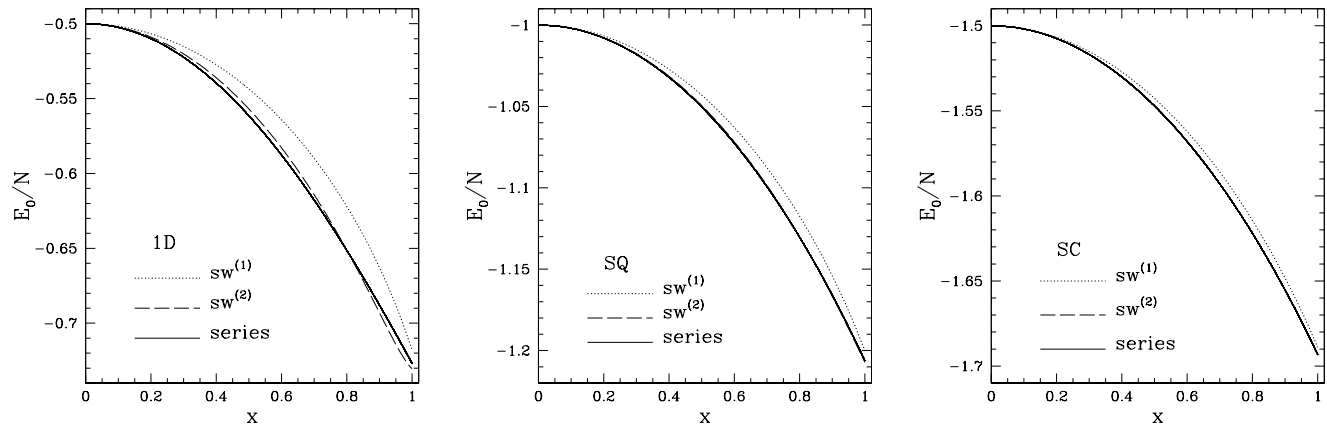


FIG. 1: Ground state energy per site for the $S = (\frac{1}{2}, 1)$ system on linear chain (a), square lattice (b) and simple cubic lattice (c). The dotted and dashed lines, in each figure are the results of first-order and second-order spin-wave theory.

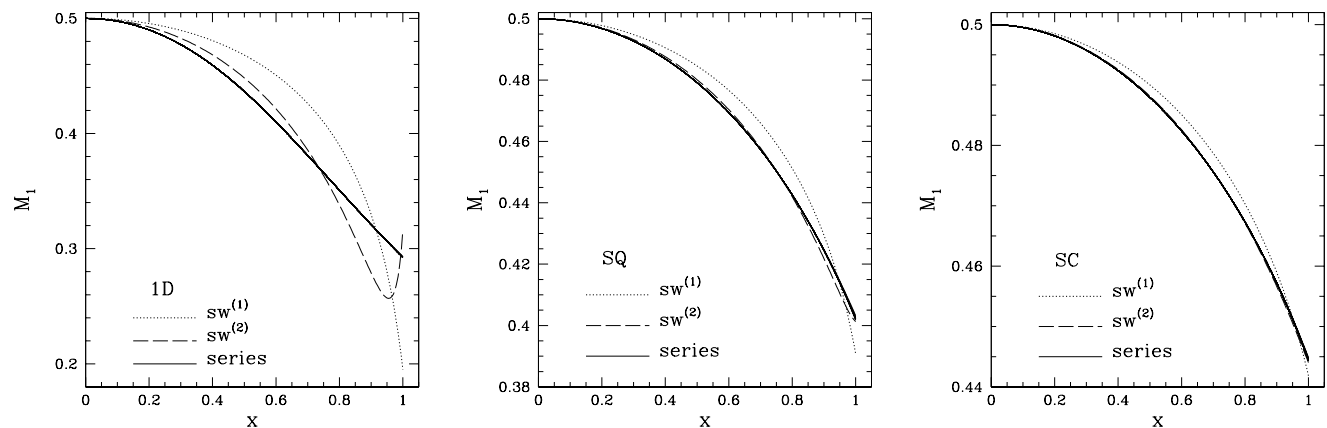


FIG. 2: Magnetization per site on the $S = \frac{1}{2}$ sublattice for the linear chain (a), square lattice (b) and simple cubic lattice (c). The dotted and dashed lines, in each figure are the results of first-order and second-order spin-wave theory.

III. RESULTS

The series can be evaluated by Padé approximants or integrated differential approximants¹⁵, either for a particular x or extrapolated to $x = 1$. We display our results in graphical form.

A. Ground state energy

Figure 1 shows the ground state energy per site, as a function of exchange anisotropy x , for the three lattices.

We note from this figure the excellent agreement between our series results and, particularly, second-order spin-wave theory. The agreement is not perfect for the chain but for $d = 2, 3$ the curves are indistinguishable on the scale of the figures. The estimated numerical error in the series is less than the width of the curve and so these results are essentially numerically exact.

Figure 2 shows the magnetization as a function of anisotropy x , again for the three lattices. Let us start from the $d = 3$ case, where spin wave theory would be expected to be most accurate. We see that this is indeed the case, and second order spin-wave theory is barely distinguishable from our series results. At the isotropic point $x = 1$ quantum

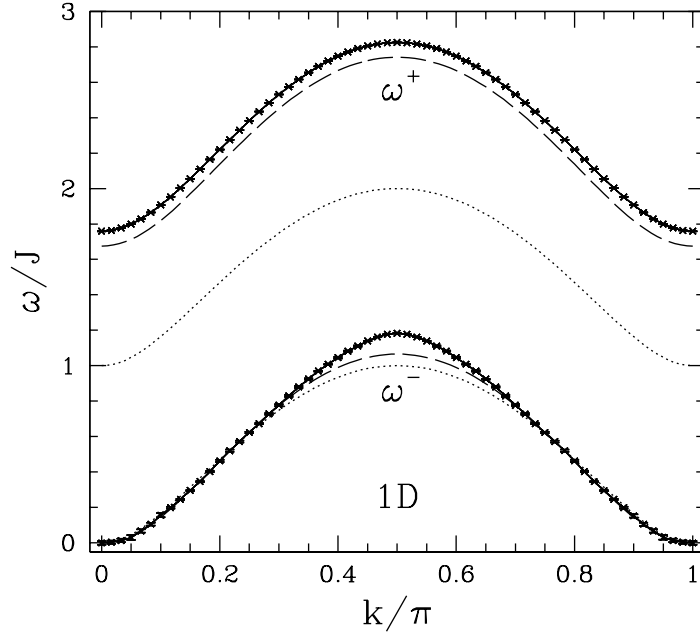


FIG. 3: Excitation energies versus k for the $s = (\frac{1}{2}, 1)$ system on the linear chain. The dotted and dashed lines give the corresponding first-order and second-order spin-wave theory.

fluctuations reduce the moment from 0.5 to 0.445, an 11% reduction (actually our numerical result is 0.44450(3)). For the square lattice quantum fluctuations reduce the sublattice moment by about 20% at $x = 1$. The series results are close to, but distinguishable from, second-order spin-wave theory. For the linear chain the differences are greater and spin-wave theory does not perform well, especially approaching $x = 1$. The series results are still very precise, and give a sublattice moment of ~ 0.29 at the isotropic point, i.e. a 40% reduce due to quantum fluctuations (the numerical value is 0.292487(6)). We note here that Tian¹⁶ has show rigorously that this system will have long range order at $T = 0$, even in 1-dimension. First-order spin wave theory overestimates the effect of quantum fluctuations near $x = 1$, while the second-order curve shows a dip and then a sharp rise near $x = 1$. This is clearly a spurious effect.

B. Excited states

Finally we turn to the excitation spectra. These are only shown for the isotropic case, $x = 1$. Figure 3 shows the two excitation branches for the chain versus k , again together with the spin-wave results. The k^2 dispersion is evident in both spin wave and series curves. Both bands have an approximante cosine shape. For the lower branch spin wave theory is quite accurate, except near $k = \frac{\pi}{2}$, but for the upper branch first-order spin-wave theory gives a large underestimate. Second-order theory is better, but still under estimates the excitation energy over the entire k range.

Figure 4 shows the dispersion curves for magnon excitation for the square lattice, along 3 lines in the Brillouin zone. In this case the series and second-order spin-wave results agree very well at all points, while the first-order spin-wave results are too low. Note the almost flat spectrum along the zone boundary from $(\pi, 0)$ to $(\pi/2, \pi/2)$. In first and second order spin-wave theory this is completely flat, as the \mathbf{k} -dependence arises from $\gamma_{\mathbf{k}} = \frac{1}{2}(\cos k_x + \cos k_y)$. The

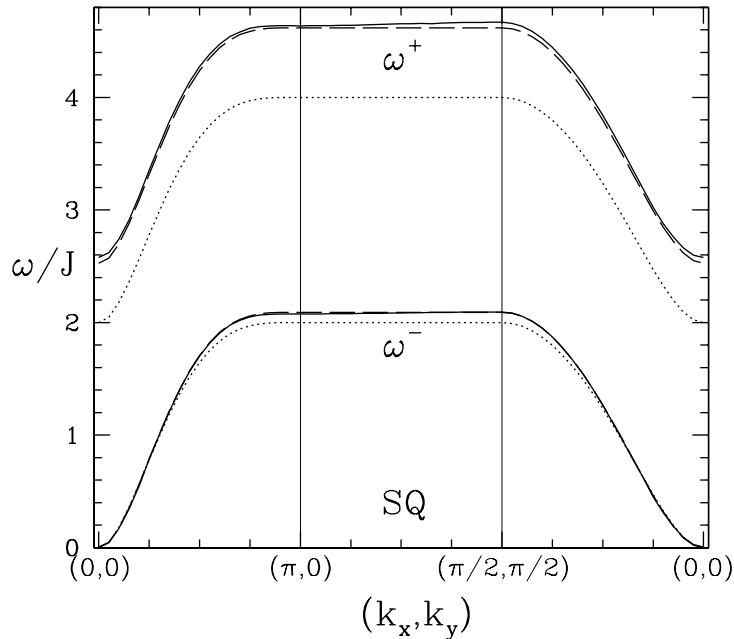


FIG. 4: Magnon dispersion curves for the $s = (\frac{1}{2}, 1)$ system on the square lattice, for special lines in the Brillouin zone. The dotted and dashed lines give the first-order and second-order spin-wave results.

series result shows a slight rise from $(\pi, 0)$ to $(\pi/2, \pi/2)$.

The corresponding results for the simple cubic lattice are shown in Figure 5, again for special lines in the zone. Agreement between series and spin-wave results is excellent, with the second order spin-wave results virtually indistinguishable from the series.

IV. CONCLUSIONS

We have used linked cluster series expansions about the Ising limit to investigate ground state properties of simple mixed spin $S = (\frac{1}{2}, 1)$ quantum antiferromagnets, on linear chain, square and simple cubic lattices. The series are very regular and easily analyzable, and we believe the results are essentially numerically exact. We have calculated the ground state energy, sublattice magnetizations, and magnon excitation spectra, and compared our results with first and second order spin wave theory. As is known from previous work on Heisenberg antiferromagnets, second-order spin-wave theory is surprisingly accurate, even in 1-dimension. In the present case the agreement is even better, as demonstrated by our results above. Presumably this reflects the fact that the ground state has a finite spin.

Our calculated excitation spectra show a quadratic dispersion at $\mathbf{k} = 0$, and we have also computed the curvature α , defined by $\omega_k^- = \alpha k^2$. In Table II we summarize all our numerical results at $x = 1$, and present a comparison with other methods.

This work demonstrates that the series method is very powerful in studying mixed spin quantum ferrimagnets, and encourages its use in more complex mixed-spin models, including, for example, frustrated systems. We are pursuing a number of calculations along these lines.

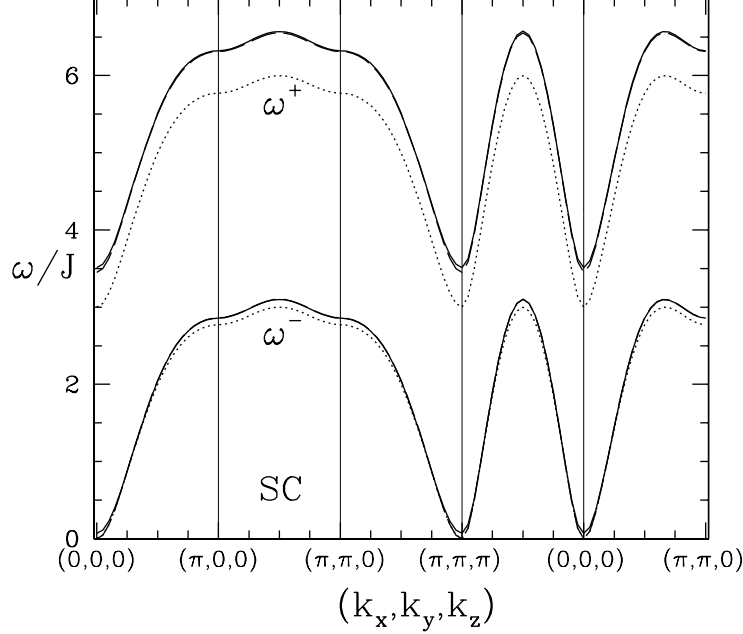


FIG. 5: Magnon dispersion curves for the $s = (\frac{1}{2}, 1)$ system on the simple cubic lattice, for special lines in the Brillouin zone. The dotted and dashed lines give the first-order and second-order spin-wave results.

Appendix

We provide, for completeness, a summary of first and second order spin wave theory for this system. Equivalent treatments have been given in Ref. 10, and elsewhere.

The Hamiltonian for the anisotropic system is (setting $J = 1$)

$$H = \sum_{\langle lm \rangle} [s_l^z S_m^z + x(s_l^x S_m^x + s_l^y S_m^y)] + h_1 \sum_l s_l^z + h_2 \sum_m S_m^z, \quad (8)$$

where we have divided the lattice sites into even and odd sublattices, denoted by l and m respectively, and introduced the magnetic fields h_1 and h_2 .

We firstly introduce boson operators a_l and b_m via the Dyson-Maleev transformation on the two sublattices:

$$\text{l - sublattice : } \quad s_l^z = S_1 - a_l^\dagger a_l, \quad s_l^+ = (2S_1)^{1/2} a_l - (2S_1)^{-1/2} a_l^\dagger a_l a_l, \quad s_l^- = (2S_1)^{1/2} a_l^\dagger, \quad (9)$$

$$\text{m - sublattice : } \quad S_m^z = b_m^\dagger b_m - S_2, \quad S_m^+ = (2S_2)^{1/2} b_m^\dagger - (2S_2)^{-1/2} b_m^\dagger b_m^\dagger b_m, \quad S_m^- = (2S_2)^{1/2} b_m.$$

Note that this transformation is not Hermitian. In terms of the boson operators, the Hamiltonian can be expressed as:

$$\begin{aligned} H = & -N(S_1 S_2 z - h_1 S_1 + h_2 S_2)/2 \\ & + (z S_2 - h_1) \sum_l a_l^\dagger a_l + (z S_1 + h_2) \sum_m b_m^\dagger b_m + x \sqrt{S_1 S_2} \sum_{\langle lm \rangle} (a_l b_m + a_l^\dagger b_m^\dagger) \\ & - \sum_{\langle lm \rangle} a_l^\dagger a_l b_m^\dagger b_m - \frac{x}{2} \sqrt{S_1 S_2} \sum_{\langle lm \rangle} (a_l^\dagger a_l a_l b_m / S_1 + a_l^\dagger b_m^\dagger b_m^\dagger b_m / S_2). \end{aligned} \quad (10)$$

Then, as in Ref. 14, we introduce the Bloch-type boson operators a_k, b_k by a Fourier transformation:

$$a_k = \left(\frac{2}{N}\right)^{1/2} \sum_l e^{ik \cdot l} a_l, \quad b_k = \left(\frac{2}{N}\right)^{1/2} \sum_m e^{-ik \cdot m} b_m, \quad (11)$$

where N is the total number of lattice sites. The quadratic part of H can be diagonalized by a Bogoliubov transformation:

$$\begin{aligned} a_k &= \alpha_k \cosh \theta_k - \beta_k^\dagger \sinh \theta_k, \\ b_k &= -\alpha_k^\dagger \sinh \theta_k + \beta_k \cosh \theta_k, \end{aligned} \quad (12)$$

where $\tanh 2\theta_k = x\gamma_k/D$, and $D = (zS_1 + zS_2 - h_1 + h_2)/(2z\sqrt{S_1 S_2})$.

With this, one can get the ground state energy up to second order in $1/S$ expansion:

$$\begin{aligned} E_h/N &= (-zS_1 S_2 + h_1 S_1 + h_2 S_2)/2 + z\sqrt{S_1 S_2} D C_1^h/2 \\ &\quad - \frac{z}{8} \left\{ [C_{-1}^h + D_0 D (C_1^h - C_{-1}^h)]^2 + x^{-2} D^2 (1 - x^2 D_0^2) (C_{-1}^h - C_1^h)^2 \right\}, \end{aligned} \quad (13)$$

where $D_0 = D(h_1 = h_2 = 0) = (S_1 + S_2)/(2\sqrt{S_1 S_2})$, $C_n^h = \frac{2}{N} \sum_{\mathbf{k}} [(1 - x^2 \gamma_{\mathbf{k}}^2 D^{-2})^{n/2} - 1]$.

Setting the external magnetic field to zero (i.e. $h_1 = h_2 = 0$), one can derive from Eq.(13) the ground-state energy E_0 :

$$E_0/N = -zS_1 S_2/2 + z(S_1 + S_2)C_1/4 - \frac{z}{8} \left\{ [C_{-1} + D_0^2 (C_1 - C_{-1})]^2 + x^{-2} D_0^2 (1 - x^2 D_0^2) (C_{-1} - C_1)^2 \right\} \quad (14)$$

where

$$C_n = C_n^{h=0} = \frac{2}{N} \sum_{\mathbf{k}} \left[(1 - x^2 \gamma_{\mathbf{k}}^2 D_0^{-2})^{n/2} - 1 \right]. \quad (15)$$

Differentiating Eq.(13) with respect to h_1 , one finds the magnetization M_1 :

$$M_1 = \frac{2}{N} \frac{\partial E_h}{\partial h_1} \Big|_{h_1=h_2=0} = S_1 - \frac{C_{-1}}{2} + \frac{C_{-3} - C_{-1}}{2x^2(S_1 + S_2)} [D_0^2(1 - x^2)(C_1 - C_{-1}) + x^2(D_0^2 - 1)C_{-1}], \quad (16)$$

Similarity, one can get M_2 , which is different from M_1 by an constant $S_2 - S_1$, as expected.

One can also get the two branches of magnon dispersion without the external magnetic field, again up to second order in a $1/S$ expansion:

$$\begin{aligned} \omega^\pm/J &= \pm z(S_2 - S_1)/2 + z(S_1 + S_2)Q_1/2 \pm \frac{D_0 z(S_2 - S_1)}{4\sqrt{S_1 S_2}} (C_{-1} - C_1) \\ &\quad - \frac{z}{2} \left[(x^{-2} - 1) D_0^2 (Q_{-1} - Q_1) (C_{-1} - C_1) + Q_1 C_1 D_0^2 + Q_{-1} C_{-1} (1 - D_0^2) \right] \end{aligned} \quad (17)$$

where $Q_n = (1 - x^2 \gamma_{\mathbf{k}}^2 D_0^{-2})^{n/2}$

For $x = 1$, we recover the second-order spin-wave results of Ivanov¹¹. It is interesting to study the asymptotic behaviour for the quantities C_n near $x = 1$. For the case $S_1 = S_2$, the leading order correction term to C_n near $x = 1$ is¹⁴ $\text{const} \times (1 - x^2)^{1/2}$, while for case $S_1 \neq S_2$, it is easy to show that the asymptotic behaviour for the quantities C_n near $x = 1$ is:

$$C_n(x) = C_n(1) + \frac{n}{2} [C_{n-2}(1) - C_n(1)](1 - x^2) + \dots \quad (18)$$

For linear chain (1D), square lattice (SQ) and simple cubic lattice (SC), C_n at $x = 1$ for $(S_1, S_2) = (1/2, 1)$ are

$$\text{1D} \quad C_1 = -0.29097039335, \quad C_{-1} = 0.60977301072, \quad C_{-3} = 5.3812664598 \quad (19)$$

$$\text{SQ} \quad C_1 = -0.13351109261, \quad C_{-1} = 0.21847549012, \quad C_{-3} = 1.3753265565 \quad (20)$$

$$\text{SC} \quad C_1 = -0.08401123644, \quad C_{-1} = 0.11629596999, \quad C_{-3} = 0.5647562506 \quad (21)$$

$$(22)$$

ACKNOWLEDGMENTS

This work forms part of a research project supported by a grant from the Australian Research Council. The computations were performed on an AlphaServer SC computer. We are grateful for the computing resources provided by the Australian Partnership for Advanced Computing (APAC) National Facility.

* w.zheng@unsw.edu.au; <http://www.phys.unsw.edu.au/~zwh>

† j.oitmaa@unsw.edu.au

- ¹ W.P. Wolf, Rep. Prog. Phys. **24**, 212(1961).
- ² P.J. Koningsbruggen, O. Kahn *et al.* Inorg. Chem. **29**, 3325(1990).
- ³ S. Pati, S. Ramasesha and D. Sen, Phys. Rev. **B55**, 8894(1997).
- ⁴ S. Yamamoto, S. Brehmer and H.J. Mikeska, Phys. Rev. **B57**, 13610(1998).
- ⁵ C. Wu, B. Chen, X. Dai, Y. Yu and Z.B. Su, Phys. Rev. **B60**, 1057(1998).
- ⁶ E. Garcia-Matres, *et al.* J. Magn. Magn. Mater. **149**, 363(1995); A. Zheludev *et al.* Phys. Rev. Lett. **80**, 3630(1998).
- ⁷ Y. Takuskima, A. Koga and N. Kawakami, Phys. Rev. B **61**, 15189(2000).
- ⁸ J. V. Alvarez, R. Valenti and A. Zheludev, Phys. Rev. **B65**, 184417(2002).
- ⁹ J.H. Park, J.T. Culp, D.W. Hall, D.R. Talham and M.W. Meisel, preprint, cond-mat/0206319.
- ¹⁰ N.B. Ivanov, Phys. Rev. **B62**, 3271(2000), and reference therein.
- ¹¹ N.B. Ivanov, J. Richter and U. Schollwock, Phys. Rev. **B58**, 14456(1998).
- ¹² N.B. Ivanov, J. Richter and D.J.J. Farnell, Phys. Rev. **B66**, 014421(2002).
- ¹³ M.P. Gelfand and R.R.P. Singh, Advances in Physics **49**, 93(2000).
- ¹⁴ W. Zheng, J. Oitmaa and C.J. Hamer, Phys. Rev. **B43**, 8321(1991); J. Oitmaa, C.J. Hamer and W. Zheng, *ibid.* **B50**, 3877(1994).
- ¹⁵ A.J. Guttmann, in “Phase Transitions and Critical Phenomena”, Vol. 13 ed. C. Domb and J. Lebowitz (New York, Academic, 1989).
- ¹⁶ G.S. Tian, Phys. Rev. **B56**, 5355(1997).

TABLE I: Series coefficients for the ground state energy per site E_0/NJ Magnetization M_1 , and two branches of magnon ω^\pm/J at $\mathbf{k} = 0$ for the linear chain, the square lattice and the simple cubic lattice. Nonzero coefficients x^r up to order $r = 22$ for 1d, order 14 for square lattice, and order 12 for simple cubic lattice are listed.

r	E_0/NJ	M_1	$\omega^-(\mathbf{k} = 0)/J$	$\omega^+(\mathbf{k} = 0)/J$
linear chain				
0	$-5.00000000 \times 10^{-1}$	$5.00000000 \times 10^{-1}$	1.00000000	2.00000000
2	$-2.50000000 \times 10^{-1}$	$-2.50000000 \times 10^{-1}$	-2.00000000	-1.00000000
4	$1.04166667 \times 10^{-2}$	$-5.90277778 \times 10^{-2}$	1.12500000	2.31250000
6	$2.56799769 \times 10^{-2}$	$2.01786748 \times 10^{-1}$	3.45052083	-5.81163194
8	$-1.40457216 \times 10^{-2}$	$-7.01659922 \times 10^{-2}$	-3.34128599	$1.92529744 \times 10^{+1}$
10	$-6.52895221 \times 10^{-3}$	$-1.51931908 \times 10^{-1}$	$-1.24692841 \times 10^{+2}$	$-7.43345195 \times 10^{+1}$
12	$1.20231578 \times 10^{-2}$	$1.67134766 \times 10^{-1}$	$9.95763258 \times 10^{+2}$	$3.08779448 \times 10^{+2}$
14	$-9.68145478 \times 10^{-4}$	$6.73415017 \times 10^{-2}$	$-3.98363592 \times 10^{+3}$	$-1.34245308 \times 10^{+3}$
16	$-1.00328363 \times 10^{-2}$	$-2.45737502 \times 10^{-1}$	$7.07316949 \times 10^{+3}$	$6.03441420 \times 10^{+3}$
18	$6.99312641 \times 10^{-3}$	$8.82808138 \times 10^{-2}$	$6.98417467 \times 10^{+3}$	$-2.78235446 \times 10^{+4}$
20	$5.40374090 \times 10^{-3}$	$2.41826850 \times 10^{-1}$	$5.10317554 \times 10^{+4}$	$1.30865902 \times 10^{+5}$
22	$-1.04177497 \times 10^{-2}$	$-2.78535289 \times 10^{-1}$	$-1.73937095 \times 10^{+6}$	$-6.25428515 \times 10^{+5}$
square lattice				
0	-1.00000000	$5.00000000 \times 10^{-1}$	2.00000000	4.00000000
2	$-2.00000000 \times 10^{-1}$	$-8.00000000 \times 10^{-2}$	-1.90000000	-1.40000000
4	$-5.22222222 \times 10^{-3}$	$-1.25320988 \times 10^{-2}$	$-1.08660714 \times 10^{-2}$	$2.88214286 \times 10^{-2}$
6	$-7.77432120 \times 10^{-4}$	$-2.94020395 \times 10^{-3}$	$-6.48931742 \times 10^{-2}$	$-3.05217039 \times 10^{-2}$
8	$-3.41477688 \times 10^{-4}$	$-1.37128294 \times 10^{-3}$	$-9.96489680 \times 10^{-3}$	$-1.95162662 \times 10^{-2}$
10	$-9.77862982 \times 10^{-5}$	$-5.45189634 \times 10^{-4}$	$-6.07211572 \times 10^{-3}$	$5.18453462 \times 10^{-4}$
12	$-4.20558132 \times 10^{-5}$	$-2.71359073 \times 10^{-4}$		
14	$-1.75132661 \times 10^{-5}$	$-1.33427314 \times 10^{-4}$		
simple cubic lattice				
0	-1.50000000	$5.00000000 \times 10^{-1}$	3.00000000	6.00000000
2	$-1.87500000 \times 10^{-1}$	$-4.68750000 \times 10^{-2}$	-2.46428571	-2.03571429
4	$-3.89229911 \times 10^{-3}$	$-4.79023836 \times 10^{-3}$	$-2.21734002 \times 10^{-1}$	$-2.12222866 \times 10^{-1}$
6	$-1.24575187 \times 10^{-3}$	$-1.91047285 \times 10^{-3}$	$-1.50472245 \times 10^{-1}$	$-1.23920805 \times 10^{-1}$
8	$-4.21416977 \times 10^{-4}$	$-9.04898794 \times 10^{-4}$	$-5.75189462 \times 10^{-2}$	$-5.89627745 \times 10^{-2}$
10	$-1.66838367 \times 10^{-4}$	$-4.59923079 \times 10^{-4}$		
12	$-7.78978452 \times 10^{-5}$	$-2.59993308 \times 10^{-4}$		

TABLE II: Series coefficients for two branches of magnon dispersion $\omega^\pm(k_x, k_y) = J \sum_{k,n,m} a_{k,n,m} x^k [\cos(mk_x) \cos(nk_y) + \cos(nk_x) \cos(mk_y)]/2$ on the square lattice. Nonzero coefficients $a_{k,n,m}$ up to order $k = 10$ are listed.

(k,n,m)	$a_{k,n,m}$	(k,n,m)	$a_{k,n,m}$	(k,n,m)	$a_{k,n,m}$	(k,n,m)	$a_{k,n,m}$
ω^-/J							
(0, 0, 0)	2.000000000	(8, 0, 2)	$3.713762427 \times 10^{-3}$	(6, 3, 3)	$-8.349006559 \times 10^{-3}$	(8, 3, 5)	$-2.354734575 \times 10^{-3}$
(2, 0, 0)	$-4.000000000 \times 10^{-1}$	(10, 0, 2)	$1.371857188 \times 10^{-3}$	(8, 3, 3)	$-2.461673445 \times 10^{-3}$	(10, 3, 5)	$-1.492768067 \times 10^{-3}$
(4, 0, 0)	$6.325595238 \times 10^{-2}$	(4, 2, 2)	$-5.812500000 \times 10^{-2}$	(10, 3, 3)	$-5.509512597 \times 10^{-4}$	(8, 2, 6)	$-1.177367287 \times 10^{-3}$
(6, 0, 0)	$-5.757990909 \times 10^{-3}$	(6, 2, 2)	$-8.531165228 \times 10^{-3}$	(6, 2, 4)	$-1.252350984 \times 10^{-2}$	(10, 2, 6)	$-1.124360790 \times 10^{-3}$
(8, 0, 0)	$-1.507778153 \times 10^{-4}$	(8, 2, 2)	$1.296551584 \times 10^{-3}$	(8, 2, 4)	$-4.921900666 \times 10^{-3}$	(8, 1, 7)	$-3.363906535 \times 10^{-4}$
(10, 0, 0)	$4.027910703 \times 10^{-4}$	(10, 2, 2)	$-7.669154691 \times 10^{-5}$	(10, 2, 4)	$-1.312852923 \times 10^{-3}$	(10, 1, 7)	$-5.883082637 \times 10^{-4}$
(2, 1, 1)	-1.000000000	(4, 1, 3)	$-7.750000000 \times 10^{-2}$	(6, 1, 5)	$-5.009403935 \times 10^{-3}$	(8, 0, 8)	$-2.102441585 \times 10^{-5}$
(4, 1, 1)	$7.619047619 \times 10^{-2}$	(6, 1, 3)	$-2.053764395 \times 10^{-2}$	(8, 1, 5)	$-3.914975780 \times 10^{-3}$	(10, 0, 8)	$-9.061290707 \times 10^{-5}$
(6, 1, 1)	$8.413191563 \times 10^{-3}$	(8, 1, 3)	$1.132685760 \times 10^{-3}$	(10, 1, 5)	$-1.582142621 \times 10^{-3}$	(10, 5, 5)	$-3.071949277 \times 10^{-4}$
(8, 1, 1)	$3.139563846 \times 10^{-3}$	(10, 1, 3)	$-6.338716677 \times 10^{-4}$	(6, 0, 6)	$-4.174503279 \times 10^{-4}$	(10, 4, 6)	$-5.119915461 \times 10^{-4}$
(10, 1, 1)	$2.939474184 \times 10^{-3}$	(4, 0, 4)	$-9.687500000 \times 10^{-3}$	(8, 0, 6)	$-8.955696061 \times 10^{-4}$	(10, 3, 7)	$-2.925665978 \times 10^{-4}$
(2, 0, 2)	$-5.000000000 \times 10^{-1}$	(6, 0, 4)	$-8.507941330 \times 10^{-3}$	(10, 0, 6)	$-6.494183735 \times 10^{-4}$	(10, 2, 8)	$-1.097124742 \times 10^{-4}$
(4, 0, 2)	$-5.000000000 \times 10^{-3}$	(8, 0, 4)	$-1.541337062 \times 10^{-3}$	(8, 4, 4)	$-1.471709109 \times 10^{-3}$	(10, 1, 9)	$-2.438054981 \times 10^{-5}$
(6, 0, 2)	$-3.672253722 \times 10^{-3}$	(10, 0, 4)	$-6.373243437 \times 10^{-4}$	(10, 4, 4)	$-7.998702769 \times 10^{-4}$	(10, 0, 10)	$-1.219027491 \times 10^{-6}$
ω^+/J							
(0, 0, 0)	4.000000000	(8, 0, 2)	$-3.881904848 \times 10^{-4}$	(6, 3, 3)	$-8.349006559 \times 10^{-3}$	(8, 3, 5)	$-2.354734575 \times 10^{-3}$
(2, 0, 0)	$1.000000000 \times 10^{-1}$	(10, 0, 2)	$2.303862243 \times 10^{-3}$	(8, 3, 3)	$-2.422897285 \times 10^{-3}$	(10, 3, 5)	$-1.498879257 \times 10^{-3}$
(4, 0, 0)	$1.112767857 \times 10^{-1}$	(4, 2, 2)	$-5.812500000 \times 10^{-2}$	(10, 3, 3)	$-4.416530724 \times 10^{-4}$	(8, 2, 6)	$-1.177367287 \times 10^{-3}$
(6, 0, 0)	$1.200877715 \times 10^{-2}$	(6, 2, 2)	$-8.773526841 \times 10^{-3}$	(6, 2, 4)	$-1.252350984 \times 10^{-2}$	(10, 2, 6)	$-1.124356167 \times 10^{-3}$
(8, 0, 0)	$2.554363932 \times 10^{-3}$	(8, 2, 2)	$3.223616293 \times 10^{-4}$	(8, 2, 4)	$-4.899434792 \times 10^{-3}$	(8, 1, 7)	$-3.363906535 \times 10^{-4}$
(10, 0, 0)	$2.741930556 \times 10^{-3}$	(10, 2, 2)	$9.155008757 \times 10^{-4}$	(10, 2, 4)	$-1.084169221 \times 10^{-3}$	(10, 1, 7)	$-5.868496963 \times 10^{-4}$
(2, 1, 1)	-1.000000000	(4, 1, 3)	$-7.750000000 \times 10^{-2}$	(6, 1, 5)	$-5.009403935 \times 10^{-3}$	(8, 0, 8)	$-2.102441585 \times 10^{-5}$
(4, 1, 1)	$8.333333333 \times 10^{-2}$	(6, 1, 3)	$-2.005399403 \times 10^{-2}$	(8, 1, 5)	$-3.948827468 \times 10^{-3}$	(10, 0, 8)	$-9.039423754 \times 10^{-5}$
(6, 1, 1)	$1.081211454 \times 10^{-2}$	(8, 1, 3)	$-1.215032805 \times 10^{-3}$	(10, 1, 5)	$-1.415199959 \times 10^{-3}$	(10, 5, 5)	$-3.071949277 \times 10^{-4}$
(8, 1, 1)	$-1.064573032 \times 10^{-3}$	(10, 1, 3)	$9.174112292 \times 10^{-4}$	(6, 0, 6)	$-4.174503279 \times 10^{-4}$	(10, 4, 6)	$-5.119915461 \times 10^{-4}$
(10, 1, 1)	$2.773744329 \times 10^{-3}$	(4, 0, 4)	$-9.687500000 \times 10^{-3}$	(8, 0, 6)	$-9.043403076 \times 10^{-4}$	(10, 3, 7)	$-2.925665978 \times 10^{-4}$
(2, 0, 2)	$-5.000000000 \times 10^{-1}$	(6, 0, 4)	$-8.144935564 \times 10^{-3}$	(10, 0, 6)	$-6.249105162 \times 10^{-4}$	(10, 2, 8)	$-1.097124742 \times 10^{-4}$
(4, 0, 2)	$-2.047619048 \times 10^{-2}$	(8, 0, 4)	$-2.188469498 \times 10^{-3}$	(8, 4, 4)	$-1.471709109 \times 10^{-3}$	(10, 1, 9)	$-2.438054981 \times 10^{-5}$
(6, 0, 2)	$9.929231541 \times 10^{-3}$	(10, 0, 4)	$-2.155536602 \times 10^{-4}$	(10, 4, 4)	$-8.049648609 \times 10^{-4}$	(10, 0, 10)	$-1.219027491 \times 10^{-6}$

TABLE III: Comparison of some numerical estimates obtained by different methods for the ground-state energy E_0/NJ , the magnetization M_1 , and the energy gap $\omega^+(\mathbf{k}=0)$, and α at $x=1$.

method	E_0/NJ	M_1	$\omega^+(\mathbf{k}=0)$	α
linear chain				
series (present work)	-0.7270467(10)	0.292487(6)	1.7591(6)	1.66(3)
DMRG ³	-0.72704	0.29248		
QMC ⁴			1.75914(1)	1.48(4)
1st order SWT	-0.718228	0.195113	1	2
2nd order SWT	-0.730420	0.316344	1.67556	1.5218
3rd order SWT ¹¹	-0.727161	0.293884		
square lattice				
series (present work)	-1.2065125(10)	0.40206(1)	2.5775(8)	1.80(4)
1st order SWT	-1.20027	0.390762	2	2
2nd order SWT	-1.20731	0.401293	2.52798	1.87255
simple cubic lattice				
series (present work)	-1.693375(7)	0.44450(3)	3.505(10)	1.69(8)
1st order SWT	-1.68903	0.441852	3	2
2st order SWT	-1.69371	0.444025	3.45069	1.95157